Computers and Concrete, *Vol. 18, No. 6 (2016) 1135-1151*
DOI: http://dx.doi.org/10.12989/cac.2016.18.6.1135

Numerical simulation of hydraulic fracturing in circular holes

Hadi Haeri[*1], Vahab Sarfarazi[2], Ahmadreza Hedayat[3] and Zheming Zhu[4]

[1]*Young Researchers and Elite Club, Bafgh Branch, Islamic Azad University, Bafgh, Iran*
[2]*Department of Mining Engineering, Hamedan University of Technology, Hamedan, Iran*
[3]*Department of Civil and Environmental Engineering, Colorado School of Mines, Golden, Colorado 80401, USA*
[4]*College of Architecture and Environment, Sichuan University, Chengdu 610065, China*

(Received April 24, 2016, Revised September 9, 2016, Accepted September 27, 2016)

Abstract. For investigating the effect of the pre-existing joints on the initiation pattern of hydraulic fractures, the numerical simulation of circular holes under internal hydraulic pressure with a different pattern of the joint distributions are conducted by using a finite element code, FRANC2D. The pattern of hydraulic fracturing initiation are scrutinized with changing the values of the joint length, joint offset angle. The hydraulic pressures with 70% of the peak value of borehole wall breakout pressure are applied at the similar models. The simulation results suggest that the opening-mode fracture initiated from the joint tip and propagated toward the borehole for critical values of ligament angle and joint offset angle. At these critical values, the crack grow length is influenced by joint ligament length. When the ligament length is less than 3 times the borehole diameter the crack growth length increases monotonically with increasing joint length. The opening-mode fracture disappears at the joint tip as the ligament length increases.

Keywords: ligament angle; pre-existing joints; opening-mode fracture; hydraulic fractures; joint offset angle

1. Introduction

In the oil and gas industry, hydraulic fracturing began in the 1930s (Grebe and Stoesser, 1983) when Dow Chemical Company discovered that down hole fluid pressures could be applied to deform the formation rock, thereby allowing more effective acid stimulation. Prior to that, a U.S. patent (Frasch 1896) on matrix acidizing referred to pumping fluid under pressure to force acid further into the rock. In the late 1800s and early 1900s, wells were stimulated using nitro-shot if needed. The first hydraulic fracturing treatment to stimulate well production was performed in Kansas in 1947 on a gas well in the Hugoton field in order to compare with the current technology of acidizing wells (Veatch *et al*. 1989).

With this technique, an interval of a borehole which is free of natural fissures is sealed off with a straddle packer system and then pressurized by injection of fluid to generate a tensile circumferential stress around the borehole (Fig. 1(a)).

[*]Corresponding author, E-mail: haerihadi@gmail.com

http://www.techno-press.org/?journal=cac&subpage=8 ISSN: 1598-8198 (Print), 1598-818X (Online)

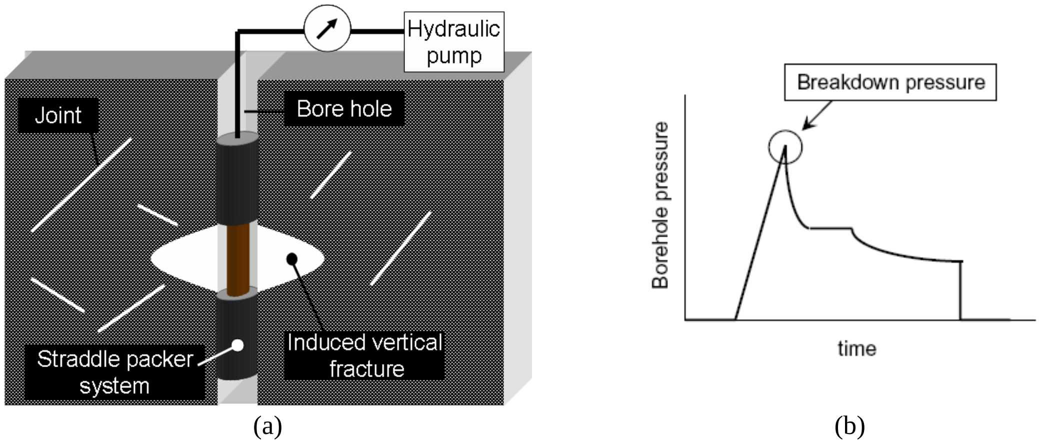

Fig. 1 (a) Set up of hydraulic fracturing and (b) detection of breakdown pressure

When this tensile stress exceeds the strength of a rock and the concentration of tectonic stresses by the borehole, fracture initiation occurs at the borehole wall. Then, breakdown pressure is observed as the borehole pressure at the fracture initiation, where the breakdown pressure is usually detected as a pressure value at the peak of borehole pressure versus time curve obtained by the in situ test (Fig. 1(b)).

Today, examples and applications of hydraulic fracturing are abundant in geomechanics. The applications of hydraulic fracturing include the disposal of waste drill cuttings underground (Moschovidis 2000), heat production from geothermal reservoirs (Pine and Cundall 1985) and fault reactivation (Board *et al*. 1992) in mining and the measurement of in situ stresses (Lamont and Jessen 1963; Desroches and Thiercelin 1993; Desroches 1995). Also hydraulic fracturing is used extensively in the petroleum industry to stimulate oil and gas wells in order to increase their productivity (Mack and Warpinski 2000).

Understanding hydraulic fracture mechanisms and then finding ways to predict the geometry of the hydraulically induced fracture and the initiation pressure are important for improving well production.

In naturally fractured reservoirs due to interaction of induced fractures with natural fractures, the fracture may propagate asymmetrically or in multiple strands or segments.
In other words, the presence of natural fractures alters the way the induced fracture propagates through the rock.

Experimental and numerical investigations (Blanton 1982; Daneshy 1974; Yang *et al*. 2004; Wong *et al*. 2006; Boutt *et al*. 2009; Zhang 2010; Liu 2010; Wangen 2011; Shimizu *et al*. 2011; Haeri 2011; Haeri and Ahranjani 2012; Lin *et al*. 2012; Wu 2013; Kresse 2013; Nagel 2013; Wu *et al*. 2013; Zhu 2013; Zhu 2014; Lin *et al*. 2014; Yu *et al*. 2014; Haeri *et al*. 2013a, 2013b; Haeri *et al*. 2014a, 2014b, 2014c; Zhu 2015; Haeri *et al*., 2015a, 2015b, 2015c, 2015d, 2015e; Haeri 2015f, 2015g, 2015h; Haeri *et al*. 2016a, 2016b) have shown that the propagating fracture crosses the natural fracture, turns into the natural fracture or, in some cases, turns into the natural fracture for a short distance, then breaks out again to propagate in a mechanically more favorable direction, depending primarily on the orientation of the natural fracture relative to stress field. Rock heterogeneity is a main cause of hydraulic fracture complexity. Hydraulic fracturing in the presence of geologic discontinuities (joints, faults, and bedding planes) is significantly different than hydraulic fracturing in homogeneous rock. Geologic discontinuities despite providing additional contact area may arrest the fracture propagation, reduce the fracture length due to fluid leakoff, reduce the total length by facilitating multiple fracture formations, and hinder proppant transport and placement (Warpinski and Teufel 1987; Potluri *et al*. 2005).

Several field and lab experimental studies have been carried out in the past to investigate the effect of natural fracture on the propagation of an induced hydraulic fracture. Warpinski and Teufel (1967) conducted experiments to study the effect of geologic discontinuities on hydraulic fracture propagation. They derived a fracture interaction criterion to predict whether the induced fracture causes a shear slippage on the natural fracture plane leading to arrest of the propagating fracture or dilates the natural fracture causing excessive leak-off.

Blair *et al*. (1989) reported the results of hydraulic fracture propagation into and through an interface, with the fracture approach angle of 90°. These results imply that high permeability streaks may not permanently stop fracture growth.

Blanton (1986) reported testing blocks of naturally fractured Devonian shale and hydrostone in which the angle of approach of the hydraulic fracture was systematically varied. These experiments showed that hydraulic fractures were unperturbed and crossed pre-existing fractures only under high differential stress conditions and high angle of approach. At intermediate and low differential stress and angles approaching the pre-existing fracture direction, the hydraulic fractures opened the pre-existing fracture and diverted the fracturing fluid or arrested propagation of the hydraulic fracture.

Reugelsdijk *et al*. (2000) performed scaled laboratory experiments on Portland cement blocks to analyze the effect of discontinuities on hydraulic fracture propagation. Also, Dong and de Pater (2001) and de Pater and Beugelsdijk (2005) carried out some numerical work based on their previous experimental work. They found that high flow rate or fluid viscosity yields fluid-driven fractures, while low flow rate just opens an existing fracture network. Many field studies (Murphy and Fehler, 1986; Britt and Hager, 1994; Vinod *et al*., 1997; Rodgerson, 2000; Azeemuddin *et al*., 2002) conducted in naturally fractured formations suggest that the effects of natural fractures on fracture propagation are enhanced fluid leak-off, premature screen-out, arrest of the fracture propagation, formation of multiple fractures, fracture offsets, high net pressures, etc.

Scan line is a commonly used method for estimating the fracture distribution on outcrops. The data obtained from the scan line method can be applied to the evaluation of hydraulic fracturing initiation in rock mass.

In this article, a series of numerical analyses was carried out in order to simulate the behavior of hydraulic crack initiation in the jointed rock mass. The novelty of this paper is to investigate the effect of the pre-existing joint distributions on the hydraulic fracturing initiation. Analyses have been performed with changing values of the joint length, the joint offset angle i.e. angle between the plane of the joint and the diametrical line that connects the inner tip of the joint to borehole wall, and ligament lengths. The effects of hydraulic pressures on hydraulic fracture initiation are also investigated.

2. Numerical simulation

A two-dimensional finite element code named FRANC2D/L (FRacture ANalysis Code for 2-D Layered structures) was used to perform the numerical modeling work. This code was originally developed at Cornell University and modified for multi-layers at Kansas State University, and is

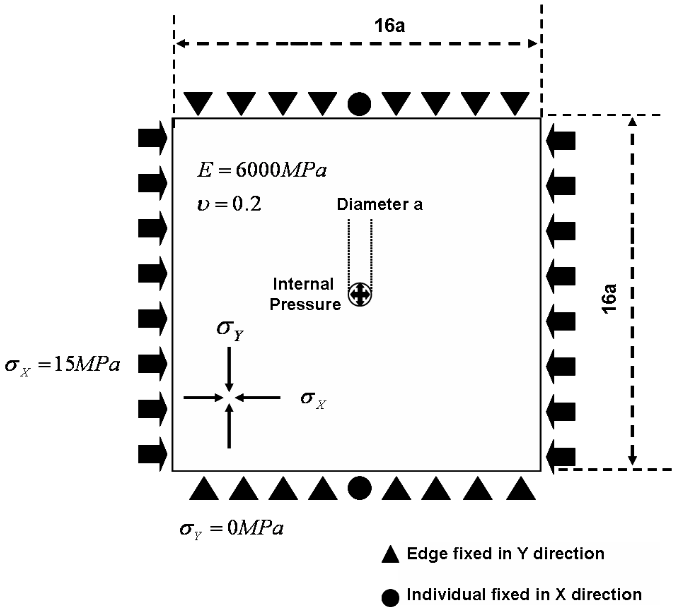

Fig. 2 A numerical model and internal pressurized hole

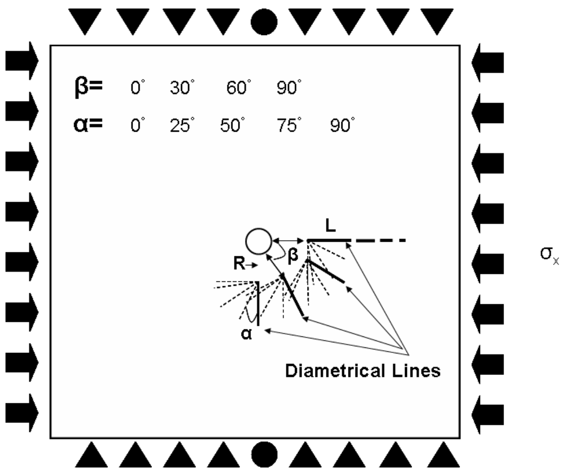

Fig. 3 A numerical model with pre-existing joint configuration

based on the theory of linear and nonlinear elastic fracture mechanics (Wawrzynek and Ingraffea, 1987). The general methodology starts with the pre-processing stage, where the geometry, mesh, material properties, and boundary conditions are defined. The modeling continues with post-processing stage where loading conditions, crack definition and crack growth process are specified.

2.1.2 Numerical model

The model and its boundary and loading conditions in the absence of a pre-existing joint are shown in Fig. 2. An internal pressure hole with diameter of a=50 cm, was centered in the model.

Table 1 Geometries used in numerical models

<table>
<tr><th>ligament Angle β (°)</th><th>Joint
Offset Angle α (°)</th><th>ligament Length</th><th>Joint
Length</th></tr>
<tr><td rowspan="9">0
30
60
90</td><td rowspan="9">0
25
50
75
90</td><td rowspan="3">a</td><td>a</td></tr>
<tr><td>2a</td></tr>
<tr><td>3a</td></tr>
<tr><td rowspan="3">2a</td><td>a</td></tr>
<tr><td>2a</td></tr>
<tr><td>3a</td></tr>
<tr><td rowspan="3">3a</td><td>a</td></tr>
<tr><td>2a</td></tr>
<tr><td>3a</td></tr>
</table>

The model dimensions were 16a × 16a. The homogeneous material with Young's modulus of 6 GPa and Poisson's ratio of 0.2 was subjected to the horizontal stress of 15 MPa and the vertical stress of 0 MPa. These principal stresses are complexly selective. The papers was establishes on these stresses. Fracture toughness value of material in numerical simulation was 1.1 MPa√m. Whereas hydraulic fracturing mode is tensile therefore its not necessary to define mode II fracture toughness in numerical modeling

Different joint configurations were placed around the wellbore (Fig. 3). The variable parameters were joint length L, ligament length R, joint offset angle of α (i.e. the angle between the diametrical line and the joint direction) and ligament angle β (i.e. the ligament angle is the counterclockwise angle between the maximum principal stress (σ_x) and the ligament length).

The ligament length (R) has a range from a to 3a with an increment of 5 mm, while the ligament angle β decreases from 90° to 0° with a negative change value of 30°. The joint offset angle of α has a range from 0° to 90°, with an increment of 25°, while joint length (L) decreases from 3a to a with a negative change value of a. Totally 180 different cases were prepared by changing the values of L, R, α and β (Table 1).

Firstly, the model behavior without pre-existing joint and internal pressure has been investigated under far field stress. Fig 4 shows the stress state around the borehole without a pre-existing joint. As can be shown there is the compressive stress concentration in upper and lower edge of internal hole while the tensile stress is generated in the right and the left edge of borehole. Secondly, the models consisting various configuration of a pre-existing joint without internal pressure have been simulated for inspection of stress state around the borehole. Runtime for each test was 5 minute. Fig. 5 shows the stress state around the borehole with presence of a pre-existing joint. In these figures the ligament angle is 0°, joint offset angle is 25°, ligament length is a and the joint length is 2a. It's clear that the pre-existing joint changes the stress state in the model so that the compressive stress is concentrated at tip of the joint while the tensile stress is disturbed on the joint faces. Also there aren't any crack initiations at tip of the pre-existing joint or at the wellbore under far field stresses. From above observations, it can be concluded that the value of the far filed stress is low enough such that it does not cause any borehole instability and/or joint dislocation/movement. Other simulations show that the joint length, ligament length, ligament angle and joint offset angle do not cause crack initiation in the absence of the internal fluid pressure.

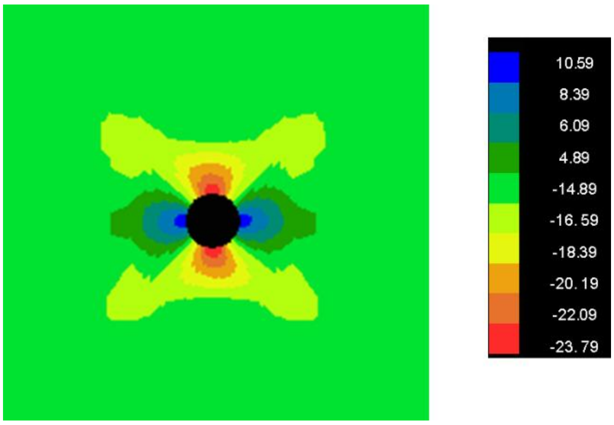

Fig. 4 The stress state around the bore hole without pre-existing joint

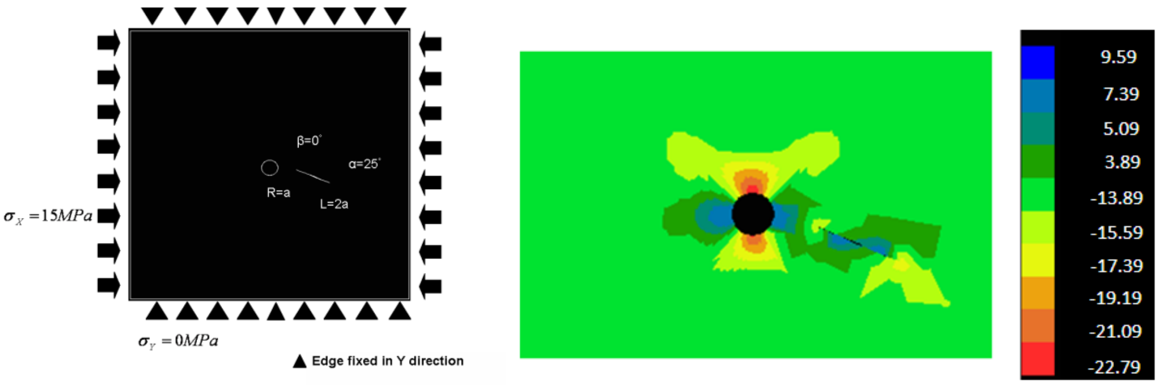

Fig. 5 The stress state around the bore hole with presence of pre-existing joint

3. Effects of the pre-existing joint on hydraulic fracturing

In order to show the coupling effect of a pre-existing joint on hydraulic fracturing, firstly a simple hydraulic fracturing without any joint was considered. As shown in Fig. 6a, the new cracks are developed hydraulically from the right and the left edge of internal hole to the direction parallel to σ_x. Even though the length of crack developed is not important in our numerical models, we are able to know that the crack length is equal to the diameter of internal hole when the internal pressure is equal to 15 MPa.

From Fig. 6(b), it's clear that the stresses at tip of the hydraulic fracture are about 0 MPa. It means that the stress concentration at the tip of the hydraulic fracture changes to zero by crack propagation. Also the stresses generated in upper and lower edge of internal hole are about 30 MPa and this value shows elastically the summation of the compressive stress concentrated at these areas by the far field stress, Fig. 5, and the compressive stress by internal pressure.

The internal pressure will be fixed at a constant value of 80% of the peak value of borehole wall breakout pressure through the entire numerical models consisting pre-existing joint and it will not be varied. 80% of the peak value of borehole wall breakout pressure is yield stress. We want to identify the crack propagation under yield stress.

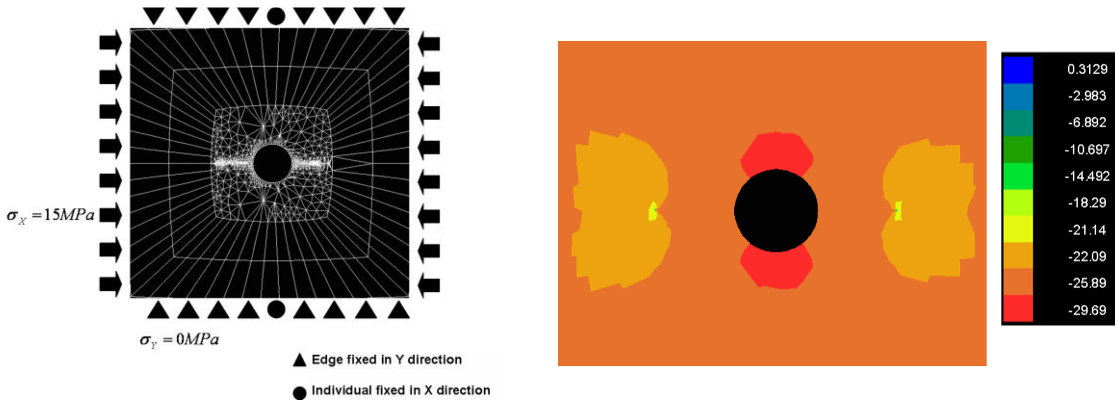

(a) (b)

Fig. 6 (a) the hydraulic fractures which develop parallel to the direction of σ_x with the length equal to the radius of the internal hole; (b) Stress state in hydraulic fracture initiation

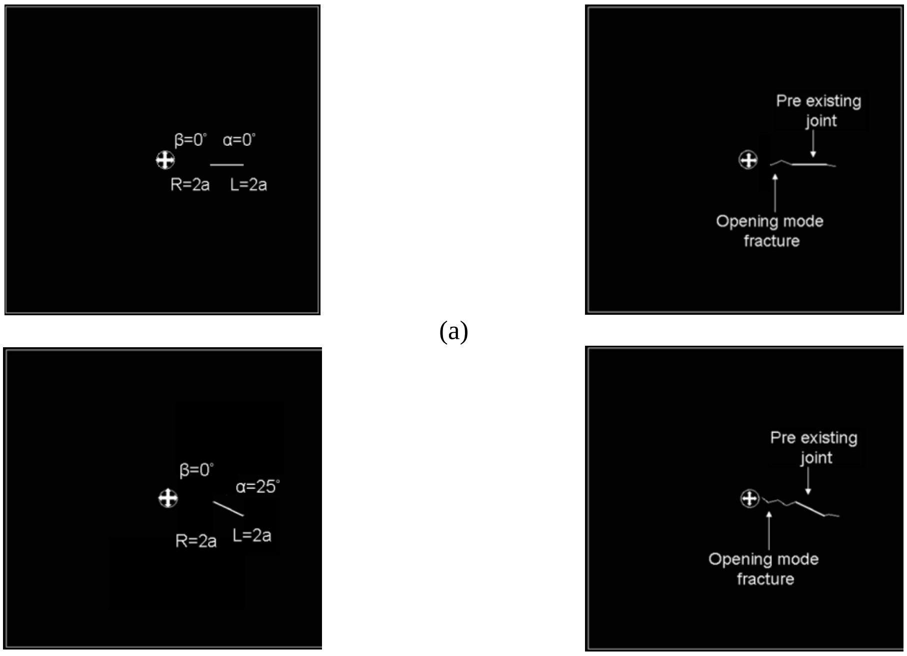

(a)

(b)

Fig. 7 The opening mode fracture initiation for two joint offset angles a: 0°; b: 25°.

After choosing the desired value of internal pressure, the effect of preexisting joint at the vicinity of the wellbore was investigated on hydraulic fracture propagation. The ligament configurations and the joint configurations have been shown in Fig. 3. The following provides a summary of representative numerical models.

a) Ligament angle is 0°:

When ligament angle is 0° and joint offset angle is less than 75° and bridge length is less than

Fig. 8 The opening mode fracture initiation for L=a.

Fig. 9 The opening mode fracture initiation for L=2a

3a, the numerical results show that the open-mode fracture was initiated at tip of the pre-existing joint and propagate toward the wellbore. In fact, in these configurations the high stress intensity was concentrated at tip of the pre-existing joint under borehole internal pressure. This stress intensity exceeds the mode-I fracture toughness and the opening mode fracture appears at the tip of the pre-existing joint.

Fig. 7(a) and (b) show the opening mode fracture initiation for two joint offset angle of 0° and 25° respectively. In these figures, the ligament angle is 0° and ligament length and the joint length are equal to 2a. As can be seen, the open-mode fracture initiates at tip of the pre-existing joint and propagate toward the wellbore. Interestingly enough, the induced crack length that has initiated at the inner tip (the tip of the joint that is close to wellbore) is longer than the length of crack that is initiated at the outer tip. The inner tip of the joint is affected by borehole pressure and the value of stress intensity factor at the inner tip is higher than that of the outer tip. This leads to further propagation of inner new crack.

The simulations also show that when the ligament length is 3a the crack isn't initiated at tip of the joint. In this condition the distance between the joint tip and the wellbore is too far such that the borehole pressure doesn't have any effect on the stress intensity at tip of the joint. Therefore the stress intensity at tip of the joint is lower than the fracture toughness and no new crack appear at tip of the joint.

Fig. 8 and Fig. 9 show the opening mode fracture initiation for two joint length of a and 2a respectively. In these figures the ligament angle is 0°, the joint offset angle is 50° and the ligament length is 2a. Close inspection of the case shows that the induced fracture length has increased with increasing the joint length.

Table 2 The results of numerical simulations for different models with ligament angle of 30°

Joint offset angle	ligament length	Joint length	Fracture grow condition	Joint offset angle	ligament length	Joint length	Fracture grow condition
		a	■			a	×
	a	2a	■		a	2a	×
		3a	■			3a	×
		a	□			a	×
0	2a	2a	□	75	2a	2a	×
		3a	■			3a	×
		a	×			a	×
	3a	2a	×		3a	2a	×
		3a	×			3a	×
		a	■			a	×
	a	2a	■		a	2a	×
		3a	■			3a	×
		a	□			a	×
25	2a	2a	□	90	2a	2a	×
		3a	■			3a	×
		a	×			a	×
	3a	2a	×		3a	2a	×
		3a	×			3a	×
		a	■				
	a	2a	■				
		3a	■				
		a	□				
50	2a	2a	□				
		3a	■				
		a	×				
	3a	2a	×				
		3a	×				

× : Fracture does not initiate at the joint tips
□ : Fracture initiates at the joint tips
■ : Fracture coalescence with the well-bore

The increase in the induced fracture length can be explained by the Fracture Mechanics Theory (Provide a reference here), which indicates that for longer fracture lengths under constant far field stress and borehole pressure, larger values of stress intensity factors at tip of the joint (KI) should be observed. This leads to longer induced fracture lengths. In case of a high stress intensity factor at tip of the joint, the newly induced crack can be extended to the wellbore.

Table 2 shows all results for fracture initiation and fracture coalescence from these numerical simulations when ligament angle is 0°.

Fig. 10(a) and (b) show the opening mode fracture initiation for two joint offset angle of 0° and 50° respectively. In these figures the ligament angle is 0°, the joint length is 2a and the ligament length is 2a. It is clear from these figures that under the same conditions, the open-mode fracture length is increased with increasing the joint offset angle. Additional simulation results also show that for the constant joint length, when the ligament length is less than 3a, the open-mode fracture growth length is increased with increasing the joint offset angle. In fact the remote stress field generates shear stress on the joint plane. This stress is intensified by the joint so that a singular stress field appears at the tips. In the plane of the initial joint, this field is predominantly shear in

(a)

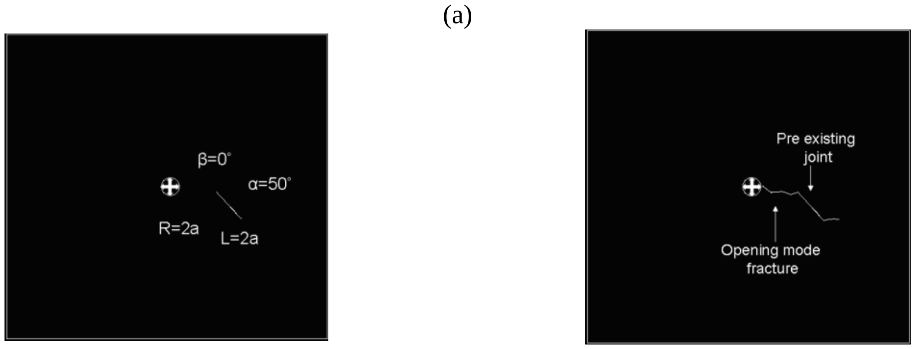

(b)

Fig. 10 The opening mode fracture initiation for two joint offset angles a: 0°; b: 50°

Fig. 11 The opening mode fracture initiation for joint offset angles of 50°.

nature; but on planes which lay at an angle to the joint tip a normal stress appears. Both of the normal stress and borehole pressure tending to cause an opening mode fracture to grow from the tips of the pre-existing joint. The introduced normal stress increases with an increase in the joint offset angle.

If ligament length is equal to the borehole diameter and/or the ratio of ligament length to joint length is less than 0.75, the open-mode fracture is connected to the wellbore in any joint offset angle. In this condition the tip of the pre-existing joint is situated in the disturbed zone around the wellbore and very high stress intensity values are obtained for the tip of the pre-existing joint. This causes an opening mode fracture to coalesce with wellbore. Fig. 11 shows the opening mode fracture coalescence to wellbore for joint offset angle of 50°. In this figure the ligament angle is 0° while the ligament length is equal to a and the joint length is equal to 2a.

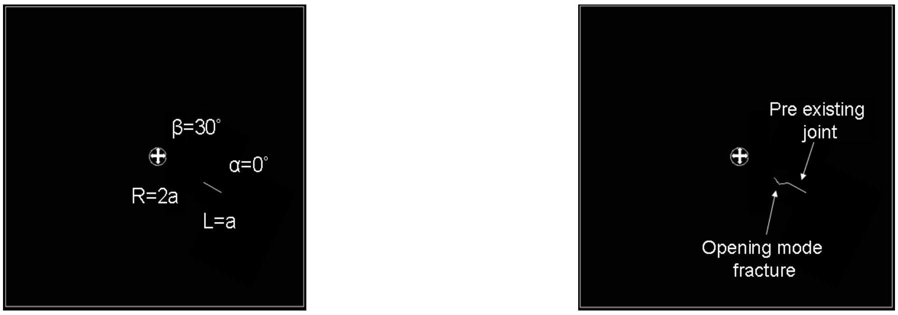

Fig. 12 The opening mode fracture initiation for Ligament angle of 30° and joint offset angles of 0°

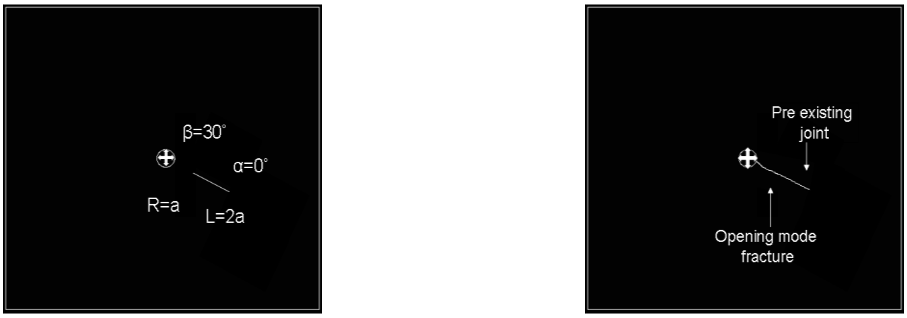

Fig. 13 The opening mode fracture initiation for two joint length; L=2a

a-2) The joint offset angle is higher than 75°:

When ligament angle is 0° and joint offset angle is higher than 75° no crack is initiated at tip of the pre-existing joint for variable joint lengths and ligament lengths. In fact, in these configurations the stress intensity at tip of the pre-existing joint isn't large enough for crack initiation.

b: ligament angle is 30°

b-1) The joint offset angle is 0°:

The numerical result show that for ligament angle of 30°, the open-mode fracture initiates at tip of the pre-existing joint and propagates toward the wellbore when joint offset angle and ligament length are 0° and less than 3a, respectively. In fact, in these configurations the high stress intensity is created at tip of the pre-existing joint due to borehole internal pressure. This stress intensity overcome to mode-I fracture toughness and the open mode fracture appears at tip of the pre-existing joint.

Fig. 12 shows the open mode fracture initiation at tip of the joint for joint offset angle of 0°. In this figure the ligament angle is 30° while the ligament length is 2a and the joint length is equal to a. As can be seen, the open-mode fracture initiates at the inner tip of the pre-existing joint and propagates toward the wellbore. This crack has stable growth and stops in the ligament because the stress intensity at tip of the joint is not high enough to cause unstable crack grow. Also the borehole pressure has minimal effect on the plane of the initial joint and therefore no tensile crack initiates at outer tip of the joint.

When the ligament length is equal to the borehole diameter, the open-mode fracture will reach the wellbore. In this condition the tip of the pre-existing joint is situated in the disturbed zone around the wellbore and very high stress intensity values exist at the tip of the pre-existing joint. This results in the coalescence of the open-mode fracture and the wellbore. Fig. 13 and Fig. 14

(a)

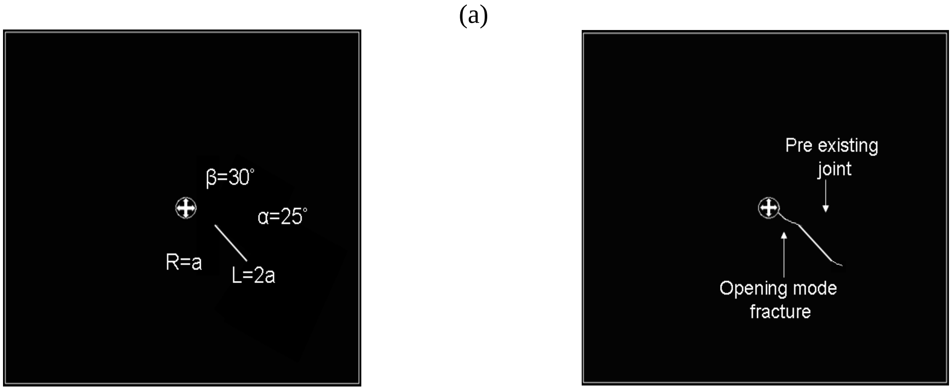

(b)

Fig. 15 The opening mode fracture initiation for two joint length; a: L=a and b: L=2a

show the opening mode fracture coalescence with wellbore for two joints with lengths of 2a and a, respectively. In these figures the ligament angle is 30°, the joint offset angle is 0° and the ligament length is equal to a. It’s clear that when ligament length is as the same as the borehole diameter the open-mode fracture reaches the wellbore.

a-2) the joint offset angle is 25°:

When the Ligament angle is 30° and the joint offset angle is 25° the open-mode fracture is coalesced with the wellbore when the ligament length is the same as the borehole diameter unless the fracture is not initiated at tip of the pre-existing joint. Fig. 15(a), (b) show the opening mode fracture coalescence to wellbore for two joint lengths of a and 2a respectively. In these figures, the ligament angle is 30°, the joint offset angle is 25° and the ligament length is equal to a. It’s clear that when ligament length is equal to the borehole diameter the open-mode fracture is connected to the wellbore.

In fact, in these configurations the high stress intensity is created at tip of the pre-existing joint due to borehole internal pressure. This stress intensity overcame the mode-I fracture toughness and the open-mode fracture appeared at tip of the pre-existing joint. The stress intensity at tip of the joint is high enough to supply the required energy for unstable crack grow so the fracture propagates unstably till it coalesces with the wellbore.

a-2) The joint offset angle is more than 25°:

When Ligament angle is 30° and joint offset angle is higher than 25°, no crack initiates at tip of the pre-existing joint, irrespective of joint length and ligament length. In fact, in these configurations the stress intensity at tip of the pre-existing joint isn’t large enough for crack

Table 3 The results of numerical simulations for different models with Ligament angle of 30°

Joint offset angle	Ligament length	Joint length	Fracture grow condition	Joint offset angle	Ligament length	Joint length	Fracture grow condition
0°	a	a	■	50° 75° 90°	a	a	×
		2a	■			2a	×
		3a	■			3a	×
	2a	a	□		2a	a	×
		2a	□			2a	×
		3a	□			3a	×
	3a	a	×		3a	a	×
		2a	×			2a	×
		3a	×			3a	×
25°	a	a	■				
		2a	■				
		3a	■				
	2a	a	×				
		2a	×				
		3a	×				
	3a	a	×				
		2a	×				
		3a	×				

× : Fracture does not initiate at the joint tips
□ : Fracture initiates at the joint tips
■ : Fracture coalescence with the well-bore

Table 4 the results of numerical simulations for different models with Ligament angle 0f 60° and 90°

Joint offset angle	Ligament length	Joint length	Fracture grow condition
0° 25° 50° 75° 90°	a	a	×
		2a	×
		3a	×
	2a	a	×
		2a	×
		3a	×
	3a	a	×
		2a	×
		3a	×

× : Fracture does not initiate at the joint tips
□ : Fracture initiates at the joint tips
■ : Fracture coalescence with the wellbore

initiation. Table 3 shows all results for fracture initiation and fracture coalescence from these numerical simulations when Ligament angle is 30°.

c: Ligament angle is more than 30°

When Ligament angle is more than 30° there is not initiated any crack at tip of the pre-existing joint for each joint offset angle, joint length and ligament length. In fact, in these configurations the stress intensity at tip of the pre-existing joint isn't enough for crack initiation. Table 4 shows all results for fracture initiation and fracture coalescence from these numerical simulations.

4. Conclusions

The numerical simulations using a two-dimensional finite element code FRANC2D/L (Fracture

Analysis Code for 2-D Layered structures) clearly indicate that the ligament angle, joint angle, ligament length and joint length affect fracture initiation and propagation at tip of the pre-existing joint significantly. Our findings are:

1-Ligament angle is 0°

1-1- joint offset angle is less than 75°

• for ligament angle of 0° when joint offset angle is less than 75° and bridge length is less than 3a, the open-mode fracture initiates at tip of the pre-existing joint and propagates toward the wellbore.

• The length of the fracture initiated from the inner tip (the tip of the joint that is close to wellbore) is longer than the length of the fracture initiated from the outer tip.

• When the ligament length is 3a the crack does not initiate at tip of the joint but when the ligament length is less than 3a the open-mode fracture growth length is increased as the joint length increases.

• The open-mode fracture growth length is increased with increasing in the joint offset angle.

• When the ligament length is equal to the borehole diameter and or the ratio of ligament length to joint length is less than 0.75, the open-mode fracture is connected to the wellbore for all joint offset angles.

1-2-Ligament angle is 0° and joint offset angle is more than 75°

• When Ligament angle is 0° and joint offset angle is higher than 75°, no crack initiates at tip of the pre-existing joint for each joint length and ligament length.

2-Ligament angle is 30°

2-2- joint offset angle is 0°:

• For Ligament angle of 30° and when joint offset angle is 0° and bridge length is less than 2a the open-mode fracture initiates at tip of the pre-existing joint and propagates toward the wellbore. The crack grows length increases with increasing the joint length.

• When ligament length is equal to the borehole diameter the open-mode fracture reaches the wellbore for any joint lengths.

2-3- joint offset angle is 25°:

• When the ligament angle is 30° and the joint offset angle is 25°, the open-mode fracture coalesces with the wellbore when the ligament length is equal to the borehole diameter otherwise the fracture does not initiate at tip of the pre-existing joint.

2-4- joint offset angle is more than 25°:

• When Ligament angle is 30° and joint offset angle is higher than 25° no crack initiation occurs at tip of the pre-existing joint for different joint lengths and ligament lengths.

3- Ligament angle is more than 30°

• When Ligament angle is more than 30°, no crack initiates at tip of the pre-existing joint for each joint offset angle, joint length and ligament length.

When ligament angle is 0°, most failures occur in rock bridge between well bore and joint.

For more accurate analysis and future studies, several factors such as the preexisting crack angle, the pre-existing crack persistency, the differentials of the remote stresses, and the variations of internal pressure should be considered.

References

Azeemuddin, M, Ghori, S.G., Saner, S. and Khan, M.N. (2002), “Injection-induced hydraulic fracturing in a

naturally fractured carbonate reservoir: a case study from Saudi Arabia", SPE 73784, presented at the SPE international symposium & exhibition on formation damage control, Lafayette, LA, 20-21 February 2002.
Blair, S.C., Thorpe, R.K., Heuze, F.E., Shaffer, R.J.(1989), Laboratory observations of the effect of geological discontinuities on hydrofracture propagation, *Proceedings of the 30th US Symposium on Rock Mechanics*, Morgantown, 433-50.
Blanton, T.L. (1982), An experimental study of interaction between hydraulically induced and pre-existing fractures. SPE 10847, *Presented at the SPE/DOE unconventional gas recovery symposium*, Pittsburgh, 16-18 May.
Blanton, T.L. (1986), Propagation of hydraulically and dynamically induced fractures in naturally fractured reservoirs, SPE 15261, *Presented at the SPE/DOE unconventional gas technology symposium*, Louisville, 18-21 May.
Board, M., Rorke, T., Williams, G. and Gay, N. (1992), Fluid injection for rockburst control in deep mining. In: Tillerson JR, Wawersik WR, editors, *Proceedings of the 33rd U.S. symposium on rock mechanics*, Rotterdam: Balkema; 111-20.
Boutt, D.F, Goodwin, L. and McPherson, B.J.O.L (2009), "Role of permeability and storage in the initiation and propagation of natural hydraulic fractures", *Water Resour Res*., **45**(5), 1-18.
Britt, L.K. and Hager, C.J. (1994), Hydraulic fracturing in a naturally fractured reservoir, SPE 28717, *Presented at the SPE international petroleum conference and exhibition*, Veracruz, Mexico, 10-13, October.
Daneshy, A.A. (1974), Hydraulic fracture propagation in the presence of planes of weakness, SPE 4852, *Presented at the SPE-European Spring Meeting*, Amsterdam, 29-30 May.
De Pater, C.J. and Beugelsdijk, L.J.L. (2005), Experiments and numerical simulation of hydraulic fracturing in naturally fractured rock, *Proceedings of the US Rock Mechanics Symposium*, Anchorage, Alaska 25-29. June.
Desroches, J. (1995), Stress testing with the micro-hydraulic fracturing technique—focus on fracture reopening. In: Daemen JK, Schultz RA, editors, *Proceedings of the 35th U.S. symposium on rock mechanics*, Rotterdam: Balkema; 217-23.
Desroches, J. and Thiercelin, M. (1993), "Modeling propagation and closure of micro-hydraulic fracturing", Int. J. Rock Mech. Min. Sci., **30(**7), 1231-1234.
Dong, C.Y. and De Pater, C.J. (2001), "Numerical implementation of displacement discontinuity method and its application in hydraulic fracturing", Comput. Method. Appl. Mech. Eng., **191**(8), 745-760.
Frasch, H. (1896), "Increasing the flow of oil-wells", U.S. Patent Number 556669, United States Patents and Trademark Office, Washington D.C.
Grebe, J.J. and Stoesser, M. (1935), Increasing crude production 20,000,000 bbl. from established fields, *World Petroleum J.*, August, 473-82.
Haeri, H. (2011), "Numerical modeling of the interaction between micro and macro cracks in the rock fracture mechanism using displacement discontinuity method", Ph.D. Thesis, Department of mining engineering, Science and Research branch, Islamic Azad University, Tehran, Iran.
Haeri, H. (2015f), "Propagation mechanism of neighboring cracks in rock-like cylindrical specimens under uniaxial compression", *J. Min. Sci.*, **51(**3), 487-496.
Haeri, H. (2015g), "Influence of the inclined edge notches on the shear-fracture behavior in edge-notched beam specimens", *Comput. Concrete*, **16**(4), 605-623,
Haeri, H. (2015h), "Experimental crack analysis of rock-like CSCBD specimens using a higher order DDM", *Comput. Concrete*, **16**(6), 881-896.
Haeri, H. and Sarfarazi, V. (2016a), "The effect of micro pore on the characteristics of crack tip plastic zone in concrete", *Comput. Concrete*, **17**(1), 107-12.
Haeri, H., Ahranjani, A.K. (2012), "A fuzzy logic model to Predict crack propagation angle under Disc Cutters of TBM", *Int. J. Academic Res.*, **4**(3),156-169.
Haeri, H., Khaloo, A. and Marji, M.F. (2015d), "A coupled experimental and numerical simulation of rock slope joints behavior", *Arab. J. Geosci.*, **8**(9), 7297-7308.
Haeri, H., Khaloo, A. and Marji, M.F. (2015e), "Experimental and numerical simulation of the microcracks

coalescence mechanism in rock-like materials", *Strength Mater.*, **47**(1), 740-754.

Haeri, H., khaloo, K. and Marji, M.F. (2015b), "Experimental and numerical analysis of Brazilian discs with multiple parallel cracks", *Arab. J. Geosci.*, **8**(8), 5897-5908.

Haeri, H., Marji, M.F. and Shahriar, K. (2015a), "Simulating the effect of disc erosion in TBM disc cutters by a semi-infinite DDM", *Arab. J. Geosci.*, **8**(6), 3915-3927.

Haeri, H., Sarfarazi, V. and Lazemi, H.A. (2016b), "Experimental study of shear behavior of planar non-persistent joint", *Comput. Concrete*, **17**(5), 639-653.

Haeri, H., Shahriar, K., Marji, M.F. and Moaref Vand, P. (2013a), Modeling the propagation mechanism of two random micro cracks in rock samples under uniform tensile loading, *Proceedings of 13th International Conference on Fracture*, China.

Haeri, H., Shahriar, K., Marji, M.F. and Moaref Vand, P. (2013b), Simulating the bluntness of TBM Disc cutters in rocks using displacement discontinuity method, *Proceedings of 13th International Conference on Fracture*, China.

Haeri, H., Shahriar, K., Marji, M.F. and Moarefvand, P. (2014a), "Investigating the fracturing process of rock-like Brazilian discs containing three parallel cracks under compressive line loading", *Strength Mater.*, **46**(3), 133-148.

Haeri, H., Shahriar, K., Marji, M.F. and Moarefvand, P. (2014b), "On the cracks coalescence mechanism and cracks propagation paths in rock-like specimens containing pre-existing random cracks under compression", *J. Central South Univ.*, **21**(6), 2404-2414.

Haeri,H., Shahriar, K., Marji, M.F. and Moarefvand, P. (2015c), "The HDD analysis of micro cracks initiation, propagation and coalescence in brittle substances", *Arab. J. Geosci.*, **8**(5), 2841-2852

Kresse, O. and Weng, X. *et al*. (2013), "Numerical modeling of hydraulic fractures interaction in complex naturally fractured formations", *Rock Mech. Rock Eng.*, **46**(3), 555-568.

Lamont, N. and Jessen, F. (1963.), "The effects of existing fractures in rocks on the extension of hydraulic fractures", *J. Petrol. Technol.*, February, 203-9.

Li, L.C., Tang, C.A., Li, G., Wang, S.Y., Liang, Z.Z. and Zhang, Y.B. (2012b), "Numerical simulation of 3D hydraulic fracturing based on an improved flow-stress-damage model and a parallel FEM technique", *Rock Mech. Rock Eng.*, **45**(5), 801-818.

Lin, P, Zhou, W.Y. and Liu, H.Y. (2015), "Experimental study on cracking, reinforcement and overall stability of the Xiaowan super-high arch dam", *Rock Mech. Rock Eng.* **48**(2), 819-841.

Liu, H., Zhang, G., Zhang, J., BIAO, F., WU, H.A. and WANG, X. (2010), "Friction loss calculation and surface pressure prediction in oil well hydraulic fracturing", *Chin. J. Rock Mech. Eng.*, **29**, 2833-2839.

Mack, M.G. and Warpinski, N.R. (2000), "Mechanics of hydraulic fracturing", *Economides, Nolte, editors. Reservoir stimulation*, 3rd ed. Chichester; Wiley, Chapter 6.

Moschovidis (2000), The Mounds drill-cuttings injection experiment: final results and conclusions, *Proceedings of the IADC/ SPE drilling conference*, 23-25, New Orleans, February, Richardson: Society of Petroleum Engineers.

Murphy, H.D. and Fehler, M.C. (1986), Hydraulic fracturing of jointed formations, *Presented at the SPE international meeting on petroleum engineering*, 17-20, Beijing, March.

Nagel, N.B., Sanchez-Nagel, M.A. *et al*. (2013), "Coupled numerical evaluations of the geomechanical interactions between a hydraulic fracture stimulation and a natural fracture system in shale formations", *Rock Mech. Rock Eng.*, **46**(3), 581-609.

Pine, R.J. and Cundall, P.A. (1985), Applications of the Fluid-Rock Interaction Program (FRIP) to the modelling of hot dry rock geothermal energy systems, *Proceedings of the international symposium on fundamentals of rock joints, Bjorkliden*, 293-302, Sweden, September.

Reugelsdijk, L.J.L, Beugelsdijk, L.J.L, de Pater, C.J. and Sato, K. (2000), Experimental hydraulic fracture propagation in multi-fractured medium, *Presented at the SPE Asia Pacific conference on integrated modeling*, 25-26, Yokohoma, April.

Rodgerson, J.L. (2000), Impact of natural fractures in hydraulic fracturing of tight gas sands, *Presented at the SPE Permian basin oil and gas recovery conference*, 21-23, Midland, TX, March.

Shimizu, H., Murata, S. and Ishida, T. (2011), "The distinct element analysis for hydraulic fracturing in hard rock considering fluid viscosity and particle size distribution", *Int. J. Rock Mech. Min. Sci.*, **48**(5), 712-727.

Veatch, R.W., Moschovidis, Z.A. and Fast, C.R. (1989), "An overview of hydraulic fracturing", Gidley, Holditch, Nierode, Veatch, editors, Recent advances in hydraulic fracturing, *Monograph*, **12,** Richardson: Society of Petroleum Engineers, 1-38.

Vinod, P.S., Flindt, M.L., Card, R.J. and Mitchell, J.P. (1997), Dynamic fluid-loss studies in low-permeability formations with natural fractures, *Presented at the SPE production operations Symposium*, 9-11, Tulsa, March.

Wangen, M. (2011), "Finite element modeling of hydraulic fracturing on a reservoir scale in 2D", *J. Pet Sci. Eng.*, **77**(3), 274-285.

Warpinski, N.R. and Teufel, L.W. (1987), "Influence of geologic discontinuities on hydraulic fracture propagation", *J. Petrol. Technol.*, **39**(02), 209-220.

Wawrzynek, P.A. and Ingraffea, A.R. (1987), "Interactive finite element analysis of fracture processes: an integrated approach", *Theo. Appl. Fract. Mech.*, **8**(2), 137-150.

Weibull, W. (1951), "Wide applicability", *J. Appl. Mech.*, **103**, 293-297.

Wong, T.F., Wong, R.H., Chau, K.T. and Tang, C.A. (2006), "Microcrack statistics, Weibull distribution and micromechanical modeling of compressive failure in rock", *Mech. Mater.*, **38**(7), 664-681.

Wu, K. and Olson, J.E. (2015), "Simultaneous multifracture treatments: fully coupled fluid flow and fracture mechanics for horizontal wells", *SPE J.*, **20**(02), 337-346.

Wu, K., Paton, D. and Zha, M. (2013), "Unconformity structures controlling stratigraphic reservoirs in the north-west margin of Junggar basin, North-west China", *Frontiers Earth Sci.*, **7**(1), 55-64.

Yang, T.H., Tham, L.G., Tang, C.A., Liang, Z.Z. and Tsui, Y. (2004), "Influence of heterogeneity of mechanical properties on hydraulic fracturing in permeable rocks", *Rock Mech. Rock Eng.*, **37**(4), 251-275.

Yu, J., Li, H., Chen, X., Cai, Y. and Mu, K. (2014), "Experimental study of permeability and acoustic emission characteristics of sandstone during processes of unloading confining pressure and deformation", *Chin. J. Rock Mech. Eng.*, **33**(1), 69-79.

Zhang, G.M., Liu, H., Zhang, J., Wu, H.A. and Wang, X.X. (2010), "Three-dimensional finite element simulation and parametric study for horizontal well hydraulic fracture", *J. Petrol. Sci. Eng.*, **72**(3), 310-317.

Zhu, H.Y,, Deng, J. *et al*. (2015), "Hydraulic fracture initiation and propagation of oil and gas wellbore with oriented perforating technique", *Rock Mech. Rock Eng.*, **48**(2), 585-601.

Zhu, H.Y., Deng, J.G., Chen, Z.J., An, F.C., Liu, S.J., Peng, C.Y.... and Dong, G. (2013), "Perforation optimization of hydraulic fracturing of oil and gas well", *Geomech. Eng.*, **5**(5), 463-483.

Zhu, H.Y., Deng, J.G., Zhao, J., Zhao, H., Liu, H.L. and Wang, T. (2014), "Cementing failure of the casing-cement-rock interfaces during hydraulic fracturing", *Comput. Concrete*, **14**(1), 91-107.

CC